

REPORT DOCUMENTATION PAGE				Form Approved OMB No. 0704-0188	
<p>maintaining the data needed, and completing and reviewing the collection of information. Send comments regarding this burden estimate or any other aspect of this collection of information, including suggestions for reducing the burden, to Department of Defense, Washington Headquarters Services, Directorate for Information Operations and Reports (0704-0188), 1215 Jefferson Davis Highway, Suite 1204, Arlington, VA 22202-4302. Respondents should be aware that notwithstanding any other provision of law, no person shall be subject to any penalty for failing to comply with a collection of information if it does not display a currently valid OMB control number.</p> <p>PLEASE DO NOT RETURN YOUR FORM TO THE ABOVE ADDRESS.</p>					
1. REPORT DATE (DD-MM-YYYY) 14-01-2002		2. REPORT TYPE Final Report		3. DATES COVERED (From - To) 14 March 2000 - 26-Mar-02	
4. TITLE AND SUBTITLE First principle calculations of electrical levels for radiation induced defects in amorphous SiO2			5a. CONTRACT NUMBER F61775-00-WE001		
			5b. GRANT NUMBER		
			5c. PROGRAM ELEMENT NUMBER		
6. AUTHOR(S) Dr. Alexander L Shlyuger			5d. PROJECT NUMBER		
			5d. TASK NUMBER		
			5e. WORK UNIT NUMBER		
7. PERFORMING ORGANIZATION NAME(S) AND ADDRESS(ES) University College London Gower Street London WC1E 6BT United Kingdom			8. PERFORMING ORGANIZATION REPORT NUMBER N/A		
9. SPONSORING/MONITORING AGENCY NAME(S) AND ADDRESS(ES) EOARD PSC 802 BOX 14 FPO 09499-0014			10. SPONSOR/MONITOR'S ACRONYM(S)		
			11. SPONSOR/MONITOR'S REPORT NUMBER(S) SPC 00-4001		
12. DISTRIBUTION/AVAILABILITY STATEMENT Approved for public release; distribution is unlimited.					
13. SUPPLEMENTARY NOTES					
14. ABSTRACT This report results from a contract tasking University College London as follows: The contractor will investigate electrical levels for radiation induced defects in amorphous SiO2. The objectives of this project are: 1) To develop an embedded cluster method for calculations of the electronic structure and spectroscopic properties as well as electron affinities and ionisation potentials of point defects in crystalline and amorphous silica; 2) To study the geometric electronic structure, stability and properties of proton and H- centres in a-quartz and a-SiO2. Details are provided in the attached statement of work.					
15. SUBJECT TERMS EOARD, Materials, Space Technology					
16. SECURITY CLASSIFICATION OF:			17. LIMITATION OF ABSTRACT UL	18. NUMBER OF PAGES 13	19a. NAME OF RESPONSIBLE PERSON Carl A. Kutsche
a. REPORT UNCLAS	b. ABSTRACT UNCLAS	c. THIS PAGE UNCLAS			19b. TELEPHONE NUMBER (Include area code) +44 (0)20 7514 4505

20020927 172

**First principle calculations of electrical levels for radiation induced defects
in amorphous SiO₂**

FINAL REPORT

A. L. Shluger and P. V. Sushko

1. Introduction

The current understanding of defects induced due to high-energy radiation in space is inadequate for making predictions about various options for device fabrication. In the past several groups have been successful in calculating ground state properties of radiation-induced defects such as hyperfine tensors measured in electron spin resonance ¹⁻³. However, the most common measurements performed during radiation testing of semiconductor devices are electrical in nature, such as capacitance-voltage, conductance-voltage, and deep-level transient spectroscopy. Thus, knowledge of electrical levels (energies in the band gap where charge states change) would be very useful, especially for cases where the nature of the defect has already been determined. So, for example, it would be very useful to know the electrical levels for the E' centers in *a*-SiO₂, as these defect have been cited as important in electron tunnelling, and as a possible electron trap ^{1, 4, 5}. In other cases, where the defect has been inferred, an accurate calculation of electrical levels could help to predict whether the defect will be observable in a spin active state, and whether multiple charge states exist in the gap. An important example of these are the various charge states of Hydrogen in SiO₂. Accurate values for these electrical levels require careful treatment of both local interactions between charge carriers and the defect, and long-range polarisation effects induced by the presence of an excess charge carrier. The former have been typically well handled through careful quantum chemical treatment of the defect and its immediate environment, either through cluster calculations, or through a supercell calculation in the neutral charge state. In the charged states, both cluster- and band structure- methods have intrinsic difficulties. The cluster methods, by themselves cannot account for long range effects. The periodic methods employ small periodic cells and must use constant background charges so that lattice sums can converge. Thus, the long-range polarisation effects are not treated well either.

Therefore the objectives of this project were: 1) To develop further an embedded cluster method where the long range polarisation effects are included explicitly and accurately; and 2) to study the geometric electronic structure, stability and properties of proton and H⁻ centres and anion vacancies in α -quartz.

2. Embedded cluster method

The embedded cluster method developed in our group and implemented in the GUESS computer code ⁶⁻⁹ allows us to study point defects in crystals and amorphous solids combining quantum mechanical treatment of atoms surrounding a defect with the shell model ¹⁰ representation of the rest of the solid. It provides the consistent Madelung potential at the site of interest and allows us to account for both ionic and electronic contributions to the polarisation of the defect environment.

In this approach, the infinite system with a single point defect is divided into several regions, as shown in Fig. 1. A spherical region I includes: i) a quantum cluster with a defect and surrounding atoms treated quantum mechanically; ii) an interface region, which connects the quantum cluster with the rest of the solid treated classically; iii) a classical region, which includes up to several hundred atoms. Region I is surrounded by a finite region II, which is treated atomistically, and region III, which is treated in the approximation of polarisable continuum. Region III conforms geometrically to the boundary between regions I and II but extends to infinity (see Fig. 1). The classical ions in regions I and II are treated in the shell model and interact between themselves via inter-atomic potentials¹¹. Both quantum and classical atoms in region I are allowed to relax in the course of calculations. Atoms in region II are kept fixed in their ideal, bulk positions and provide correct variations of the electrostatic potential inside the region I. Region III is used to calculate the polarisation energy of the infinite lattice due to the presence of a defect in region I using the Mott-Littleton approach. Our setup is very similar to the original Mott-Littleton method of calculating point defects in polar solids¹². It has then been refined in GULP¹³ and similar atomistic codes, as well as in the ICECAP embedding scheme^{14, 15}. The original computation scheme implemented in GUESS and applied to defect studies in ionic crystals has been described in refs.^{6, 9, 16}. One of its main advantages is that it allows us to calculate forces on quantum mechanical and classical ions and simultaneously optimise their positions using an effective energy minimisation scheme.

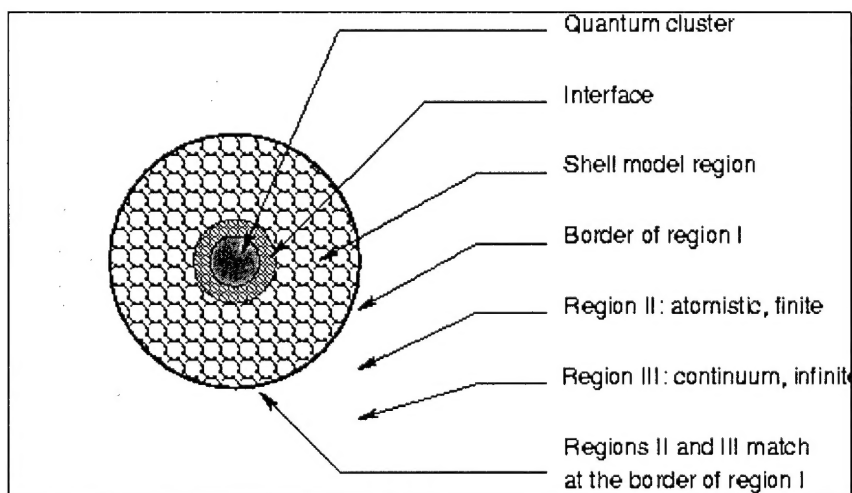


Figure 1. General setup used for the embedded cluster calculations using GUESS. See text for details.

In this project, for the first time, we apply this scheme to an ionic-covalent system, α -quartz, which has directed bonds. Such systems present a challenge for cluster calculations due to the dangling bonds formed at the cluster border. The electronic states associated with these bonds strongly perturb the cluster electronic structure and make it a poor mimic of an infinite system. To avoid problems associated with the dangling bonds, the latter have to be saturated. Usually real or pseudo-Hydrogen atoms are used for this purpose. This method is discussed in detail in ref. 17. Our approach is different in that it embeds a quantum (QM) cluster into a continuous crystal instead of treating it as a molecule. Therefore the interface atoms play a special role in this procedure as described below.

All QM clusters in our calculations are coupled with the classical environment via Si atoms, which satisfy the following condition: one neighbouring O atom always belongs to the QM cluster and the other three neighbouring O atoms belong to the classical environment. QM clusters built following this rule are always stoichiometric. These interface Si species are called pseudo-Si atoms (Si^*) and perform dual functions, as illustrated in Fig. 2.

For the electrons and cores inside the QM cluster they look like a one-electron atom with the effective charge equal to that on a regular lattice Si atom and an sp orbital centred on it. Since effective charges on Si atoms in quartz are about $+2.4 |e|$ (e is the electron charge) it represents a strong attractive centre for cluster electrons. To compensate locally the resulting strong electrostatic potential, an effective repulsive electronic potential $V(r) = A \times \exp(-Br)$ is added to mimic a screening of the Si^* core potential by valence electrons. The parameters of this potential and of the basis set for the Si^* atoms were optimised to satisfy the following conditions. i) The electronic charge is evenly distributed within the QM cluster or, in other words, the effective charge modulus on Si^* is approximately equal to $1/4$ of that on regular quantum Si atoms and $1/2$ of that on quantum O atoms. ii) The electronic states associated with Si^* atoms do not have substantial contributions at the top of the valence band or at the bottom of the conduction band. The short-range interaction between the boundary Si^* atoms and their nearest Oxygen neighbours in the QM cluster is modelled using a Morse-type classical potential, which ensures a good approximation of the inter-atomic distance between the two species. This approach effectively describes one $Si^* - O$ bond directed inside the QM cluster (see Fig. 2).

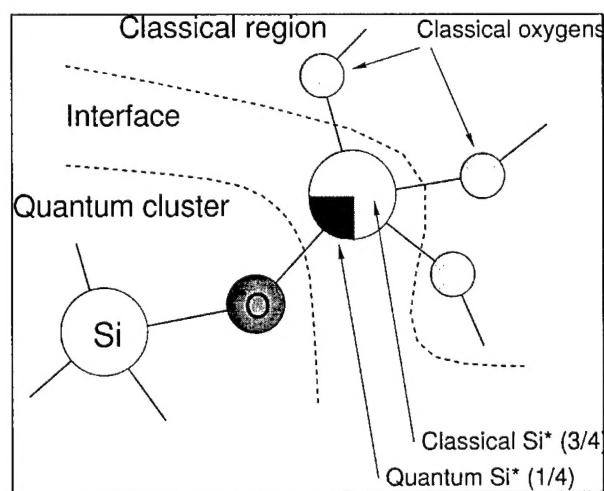


Figure 2. Model for the interface between the quantum mechanical cluster and the classical environment. The boundary Si^* atom is split into quantum mechanical and classical parts.

A second function of Si^* atoms is to interact with the shell-model ions outside the QM cluster. This interaction has Coulomb and short-range components. The interaction of point charges representing cores and shells of classical ions in regions I and II with the electron on the sp -orbital of Si^* is included in the Fock matrix via the matrix elements of the same type as the electron-nuclei interaction. In addition, these ions interact classically with the $3/4$ th of the effective charge of the classical Si ion also centred on Si^* . Thus Si^* might be envisaged as comprising $1/4$ from quantum parts and $3/4$ from classical parts (see Fig. 2). Note that the effective charge of Si^* can vary, as it depends on the population of its sp -orbitals. The short-range terms are described by inter-atomic potentials¹¹. These, originally rigid ion potentials, were modified by including shells on Oxygen ions. They are also used in order to describe the interactions between the classical atoms in region I and between the classical and quantum atom. The latter are introduced in order to mimic the exchange and resonance component of the interaction between the classical and quantum atoms across the QM cluster boundary. The expression for the total energy of the system is given in Appendix A.

The electrostatic potential produced by classical ions in regions I and II depends on their effective charges, which are parameters of inter-atomic potentials. The potentials¹¹ used in this work have been fitted using fractional ionic charges ($Q_{\text{Si}} = 2.4 e$, $Q_{\text{O}} = -1.2 e$) to reproduce accurately several of the SiO_2 polymorphs. These ionic charges have been obtained from *ab initio* calculations of small clusters using the 6-31G* basis set¹¹. As is shown below, these charges are fairly close to those obtained in our embedded cluster calculations using Natural Population Analysis (NPA)¹⁸. The latter depend, however, on a basis set. In a fully consistent approach, the charges on ions in QM cluster and these on classical ions in the perfect lattice should be the same. In the present work we tried many different basis sets and this condition is not fully satisfied for all of them. Nevertheless we believe that this does not affect our qualitative conclusions regarding the extent and character of the lattice relaxation around the defect.

Region I+II may have different shapes, but should be neutral and have zero total dipole moment. To build this region we used $\text{Si}(\text{O}_{1/2})_4$ units, which provide convenient stoichiometric elements with a very small (often practically zero) dipole moment. With this choice, a spherical region I+II gives the fastest convergence for the electrostatic potential. In our present calculations, region I+II has radius 30 Å and contains 9270 atoms. The finite size of the system results in a spread of the electrostatic potential at atomic sites, which should be equivalent in the infinite crystal. For the region I+II used in this work, the spread of the potential within the region I was less than 0.01 eV, which indicates that the system was large enough to model the infinite crystal. In most calculations discussed below the region I had the radius of 13.07 Å and contained 718 atoms.

Because region II remains fixed, its geometric structure can affect the positions of atoms in region I and in the QM cluster when they have been allowed to relax in defect calculations. In building region I+II one has a choice of the experimental structure or those determined in shell-model and quantum-mechanical calculations of the perfect system in periodic model. These structures differ slightly and we checked the effects of these differences on defect properties. For that purpose we performed periodic calculations using the GULP code¹³ and optimised the geometry of α -quartz with the pair-potentials¹¹. Then the region I+II was built using these geometric parameters and the defect structure and formation energy were calculated. The same procedure was repeated using the best α -quartz structure found in the Hartree-Fock CRYSTAL calculations¹⁹. The thus calculated formation energies differ by less than 0.03 eV. The shell-model ions in perfect α -quartz are polarised, i.e. positions of ionic shells differ from positions of cores, which results in a small dipole being associated with each ion. We have also checked that these small dipoles do not affect the results of defect calculations and one can treat region II in a point ion model.

The GUESS code provides an effective interface between the classical treatment of the rest of the system and the quantum mechanical treatment of QM cluster using the Gaussian98 code²⁰. The electronic structure of QM clusters was calculated using the Unrestricted Hartree-Fock (UHF) method and different standard basis sets ranging from STO-3G to 6-311G* for both Silicon and Oxygen atoms. QM clusters of different sizes and topology have been considered in this project: $\text{Si}_2\text{O}_7\text{Si}^*_{\text{6}}$ (cluster#1), $\text{Si}_8\text{O}_{25}\text{Si}^*_{18}$ (cluster#2), $\text{Si}_{10}\text{O}_{30}\text{Si}^*_{20}$ (cluster#3), and $\text{Si}_{18}\text{O}_{49}\text{Si}^*_{26}$ (cluster#4) with the Oxygen atom in the centre (see Fig. 3). Note that all these clusters are stoichiometric, i.e. the ratio of the numbers of Oxygen and Silicon atoms (Si^* being $\frac{1}{4}$ of a Silicon atom as discussed above) is equal to 2. Indeed, each boundary Si^* atom is treated as a $\text{Si}_{1/4}$ species and, therefore, each cluster can be viewed as built from $\text{Si}_{1/4}\text{O}_{1/2}$ bond-like elements, which are stoichiometric. When increasing the cluster size we aimed to satisfy the additional criterion that the cluster must be compact. The compactness of a given cluster can be defined as the ratio $\eta = N_{\text{cluster}}/N_{\text{crystal}}$, where N_{cluster} is the sum of quantum mechanically treated nearest neighbours for each atom in the cluster and N_{crystal} is the sum

of all nearest neighbours of the cluster atoms in the crystal. For the infinitely large cluster $\eta = 1$; for the clusters used in the present study, η increases from 0.58 for the cluster#1 to 0.72 for the cluster#4.

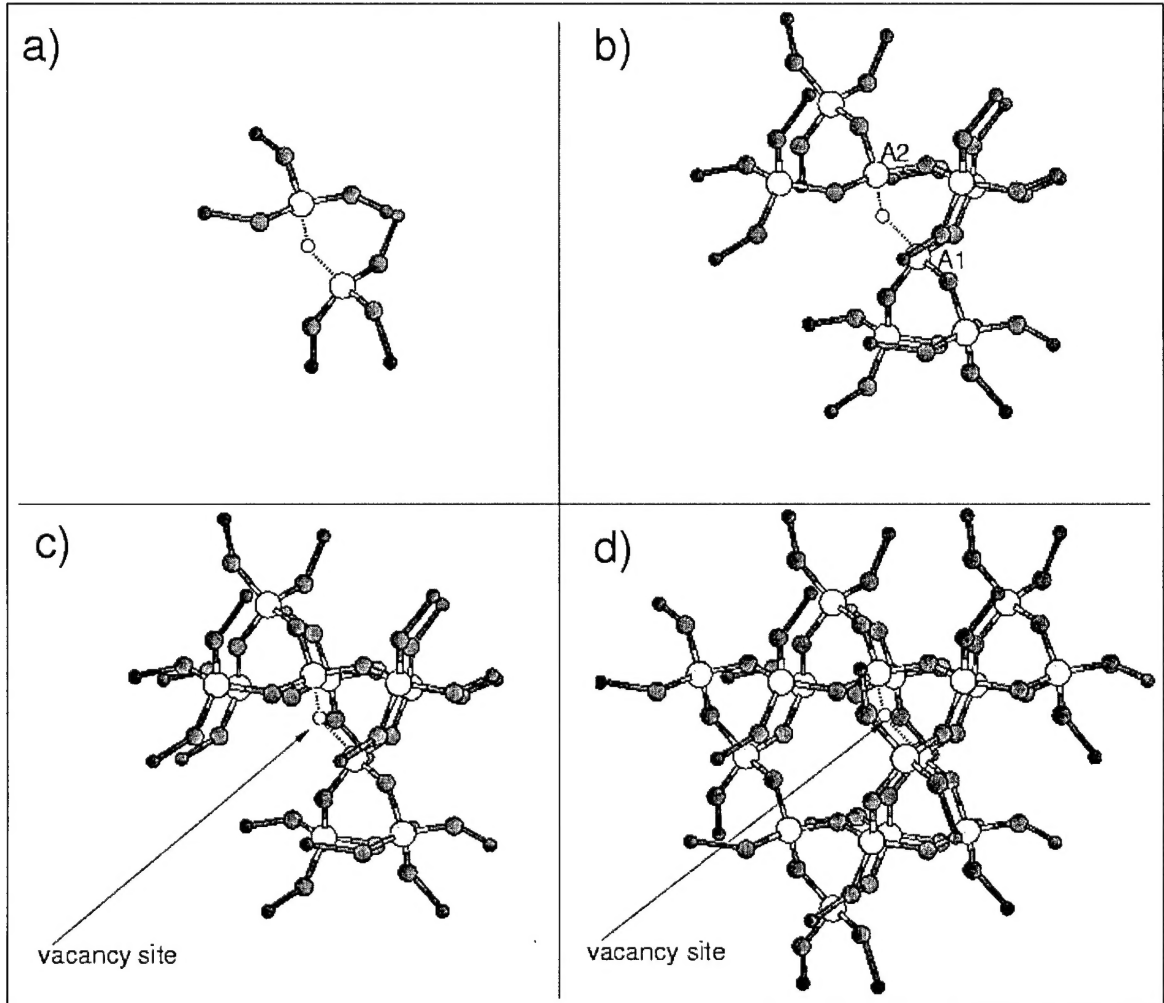


Figure 3. Quantum-mechanical clusters used in the calculations of the neutral Oxygen vacancy (shown in the same projection). a) $\text{Si}_2\text{O}_7\text{Si}^*_6$; b) $\text{Si}_8\text{O}_{25}\text{Si}^*_{18}$; c) $\text{Si}_{10}\text{O}_{30}\text{Si}^*_{20}$; d) $\text{Si}_{18}\text{O}_{49}\text{Si}^*_{26}$. Additionally, all figures show the vacancy site (empty circle), b) shows Si atoms A1 and A2, which form Si-Si bond after the vacancy is relaxed (see also Figs. 6 and 7).

To test our embedding scheme we carried out so called “perfect lattice test” calculations for each cluster. In these calculations a non-defective QM cluster was embedded in the rest of the lattice and the whole system was allowed to relax. In the case of ‘ideal’ embedding, no atoms in region I should displace from their original sites. In practice, we observed a relatively small relaxation associated with the interface region, where the maximum displacements of atoms, changes in the inter-atomic distances, and changes of the “soft” Si - O - Si angles with respect to their original values were less than 0.15 Å, 4%, and 5% respectively. Distortions in the rest of the system were at least 3 times smaller. We also checked that after relaxation the electronic structure of the cluster did not undergo any noticeable modification, i.e. there was no change in electron density distribution within the QM cluster or in the density of states.

3. Results of calculations

The technique described above was applied to theoretical modelling of Hydrogen centres and neutral Oxygen vacancy in α -quartz. Two types of Hydrogen centres were investigated: i) an H^+ centre or a proton, and ii) an H^\cdot centre. These calculations were performed using an embedded cluster $Si_5O_{16}Si^{*}_{12}$ similar to the cluster shown in Fig. 3(b) and cc-pVDZ basis for Hydrogen ion and 6-31G basis for Si and O atoms. The geometry optimisation demonstrates that the H^+ ion gets attached to a bridging Oxygen species, whereas a negative H^\cdot ion prefers to be strongly attached to a framework Si atom. The local atomic structures of these centres are shown in Figs. 4 and 5. One of the aims of this part of the project was to test the performance of the new technique before applying it to more complex systems. Therefore we have calculated the geometric structures of both centres and compared the results with the recent periodic Density Functional Theory (DFT) calculations of these centres ²¹. The H^+ and H^\cdot defects are thought to be responsible for electron charge transfer within semiconductor devices. Therefore, we have also calculated the electronic properties associated with ionisation and attachment of an additional electron to the H^\cdot and H^+ centres, respectively

H^+ centre. The optimised geometry for the H^+ centre is similar to the results of previous theoretical studies. The proton is attached to the bridging Oxygen so that thus formed OH species is oriented towards the main α -quartz channel (see Fig. 4). The character of the electron density redistribution suggests that about 0.4 of an electron is transferred to the proton forming an OH bond. Further analysis of the molecular orbitals of this system provides an additional evidence for the bond formation. Comparison of the local atomic structure with the results of the recent periodic DFT calculations ²¹ (see Table 1) demonstrates that they are almost identical. We should note that the DFT calculations were made in a 72 atom periodic cell whereas our calculations are performed in a three times smaller cluster, which treats quantum-mechanically only the local defect structure. Therefore this agreement demonstrates a good quality of the embedding potential.

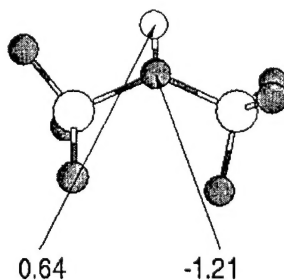


Figure 4. Local geometry and charge distribution (atomic charges of H and O atoms are shown) for the H^+ centre in α -quartz. See also Table 1.

The calculations show that H^+ centres have a positive electron affinity (EA) and thus can serve as electron traps. The electron affinity is difficult to measure experimentally and therefore accurate theoretical predictions are important. The calculated vertical EA depends on the method of calculations. We have studied the effect of the crystalline environment and the lattice polarisation on the calculated EA. Our results demonstrate that i) a molecular cluster model, which fully neglects the long-range crystalline environment of the centre, gives an electron affinity of only 0.7 eV; ii) if the

crystalline potential is correctly accounted for, the EA increases to 2.5 eV; and iii) the EA further increases to 3.0 eV if the electronic part of the lattice polarisation is taken into account.

H⁻ centre. The H⁻ centre consists of a negative Hydrogen ion attached to a Si ion making it five-fold co-ordinated. The attached H⁻ ion causes the strong reorientation of four Si – O bonds of the non-defective SiO₄ tetrahedron. In the relaxed configuration the Hydrogen ion occupies a site in the plane of the central Si and two equatorial Oxygen atoms, O_{eq} (see Fig. 5). Two other (axial) Oxygen atoms, O_{ax}, relax so that the O_{ax} – Si – O_{ax} angle is much larger than the typical angle within an ideal SiO₄ tetrahedron unit in SiO₂ polymorphs. The details of the local atomic structure are summarised in Table 1. Comparison with the periodic DFT calculations²¹ suggests that the two different approaches give the same configuration and very similar inter-atomic distances and angles with the exception of the Si – O_{eq} distances. The charge density redistribution is such that more than 0.6 electron is transferred from the H⁻ ion, which indicates formation of a Si – H bond. The calculated ionisation potential for the H⁻ centre is equal to 3.4 eV.

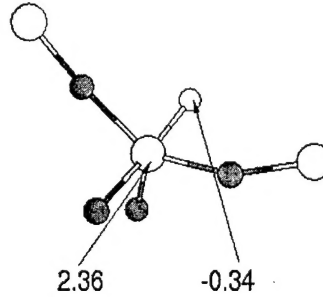


Figure 5. Local geometry and charge distribution (atomic charges of H and Si atoms are shown) for the H⁻ centre in α -quartz. See also Table 1.

Table 1. Parameters of the local geometry of the H⁺ and H⁻ defects in α -quartz.

H ⁺ centre	This work	Ref. [21]
Dist(H-O), Å	0.983	1.017
Dist(O-Si), Å	1.775	1.773
Ang(Si-O-Si), deg	135.2	134.5
H ⁻ centre	This work	Ref. [21]
Dist(H-Si), Å	1.456	1.508
Dist(Si-O _{ax}), Å	1.784	1.757
Dist(Si-O _{eq}), Å	1.697	1.994
Ang(O _{ax} -Si-O _{ax}), deg	169.8	170.0
Ang(O _{eq} -Si-O _{eq}), deg	106.2	106.0

Oxygen vacancy. We performed extensive calculations of the structure and properties of neutral Oxygen vacancy in α -quartz using the embedded cluster technique described above. The dependence of the vacancy structure, formation energy, lattice relaxation, and optical excitation energies on the quantum cluster size and on the basis set have been studied. Full details of these calculations are described in ref. 22. They were performed for the four quantum clusters shown in Fig. 3. All calculations included a counterpoise correction for the basis set superposition error (BSSE)²³ (see also recent discussion in ref. 24). This means that the Oxygen basis set remained centred in the vacancy when an Oxygen atom was removed to form a vacancy. Similarly, the Oxygen atom energy was calculated including the basis sets of all other atoms in each particular QM cluster centred at the positions of these atoms around the vacancy.

The calculated properties of the Oxygen vacancy include the formation energy, the Si-Si distance, the position of the one-electron vacancy level with respect to the highest orbital of the valence band, and the charge redistribution within the vacancy. The dependence of these properties on the flexibility of the basis set was investigated for several basis sets (STO-3G, 3-21G, 6-21G, 6-31G with and without polarisation functions) and their combinations for Si and O atoms using QM cluster $\text{Si}_2\text{O}_7\text{Si}^*_6$. The calculated values vary considerably and do not demonstrate a tendency to the saturation. These variations are difficult to rationalise but we believe they originate from two sources: i) too narrow basis set, and ii) small QM cluster used in our calculations.

We have also studied the dependence of the vacancy formation energy on the cluster size and details of the cluster geometry. For that a QM cluster was relaxed using small basis set, e.g. STO-3G, then the relaxed geometry and a more flexible basis set, e.g. 6-31G, were used for a single point energy calculation. The calculated formation energies show little dependence on the cluster geometry. In other words, one could relax geometry of the vacancy using a small basis set and then calculate the formation energy using the same geometry and a larger basis set without making a significant error. This result is expected to be general for localised defects and can help us to achieve reasonable compromise between the accuracy and CPU-time requirements of further calculations. We suggest that geometry of localised defects can be, with a good accuracy, calculated using 3-21G and 6-31G basis sets. To obtain more accurate electronic structure 6-31G* and 6-311G* basis sets can be used.

We have found that, irrespective to the cluster size and basis set used in the calculations, the neutral Oxygen vacancy in α -quartz induces very strong and anisotropic lattice distortion, which extends further than about 13 Å from the vacant site (see Fig. 6). For comparison, the relaxation of atoms surrounding a neutral vacancy in some other oxides, such as ZrO_2 and MgO , is much smaller. This results from different structure and chemical bonding in these materials. In particular, in MgO unlike α -quartz the Oxygen site is the centre of inversion. The peculiar structure of α -quartz is also manifest in the strong asymmetry of the relaxation of the two Si atoms neighbouring the vacancy (Figs. 6 and 7).

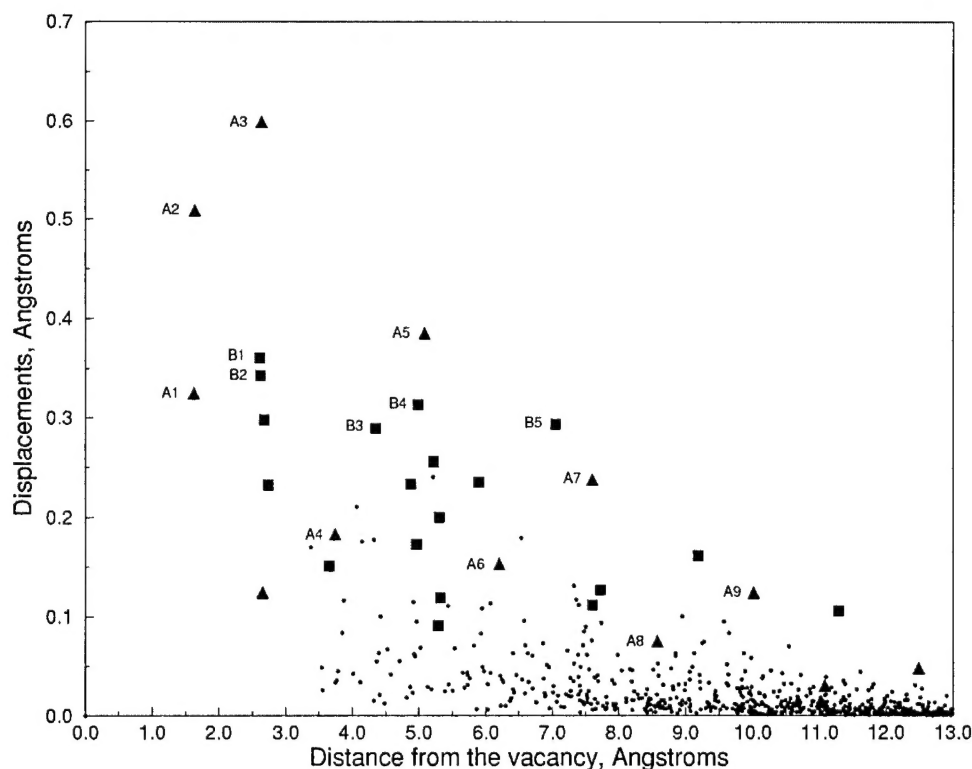


Figure 6. Total displacements of atoms resulting from the relaxation of the neutral Oxygen vacancy. Atoms participating in the relaxation of A- and B-types are shown as triangles and squares respectively. Notations correspond to those in Figs. 7 and 3(b).

With full relaxation, the equilibrium distance between the two Si atoms is equal to 2.36 Å, essentially identical to the Si-Si spacing in elemental silicon. These values remain practically the same for larger clusters calculated in the same basis set. The results suggest that the rest of the lattice allows the Si atoms to relax without serious inhibition, driven by bond formation. Nevertheless, their strong displacement induces a complicated distortion of the whole region I. The atomic displacements decrease for distant atoms, but the number of these atoms increases rapidly and the resulting effect on defect properties is not negligible. The absolute values of atomic displacements from the perfect lattice sites as a function of their distance from the vacant oxygen site are presented in Fig. 6. One can clearly see that displacements decrease to almost zero values (0.01 Å) only at the outer boundary of region I (13.07 Å). They are still about 0.2 - 0.4 Å at 5 Å from the vacant site (the 6th neighbouring shell) and are not negligible even at 10.0 Å from the vacancy. Further analysis of the character of atomic displacements demonstrates that they can be clearly divided into two types shown in Figs 6 and 7 (a,b). Type A is extremely anisotropic due to the absence of the centre of inversion in quartz. It involves large displacements of the silicon and oxygen atoms directed towards the vacancy approximately along the line connecting the two Si atoms neighbouring the vacancy. The displacements of the silicon atoms, A1,2,4,6,8 are smaller and die much more rapidly than these of the oxygen atoms marked as A3,5,7,9 in Figs. 6 and 7a.

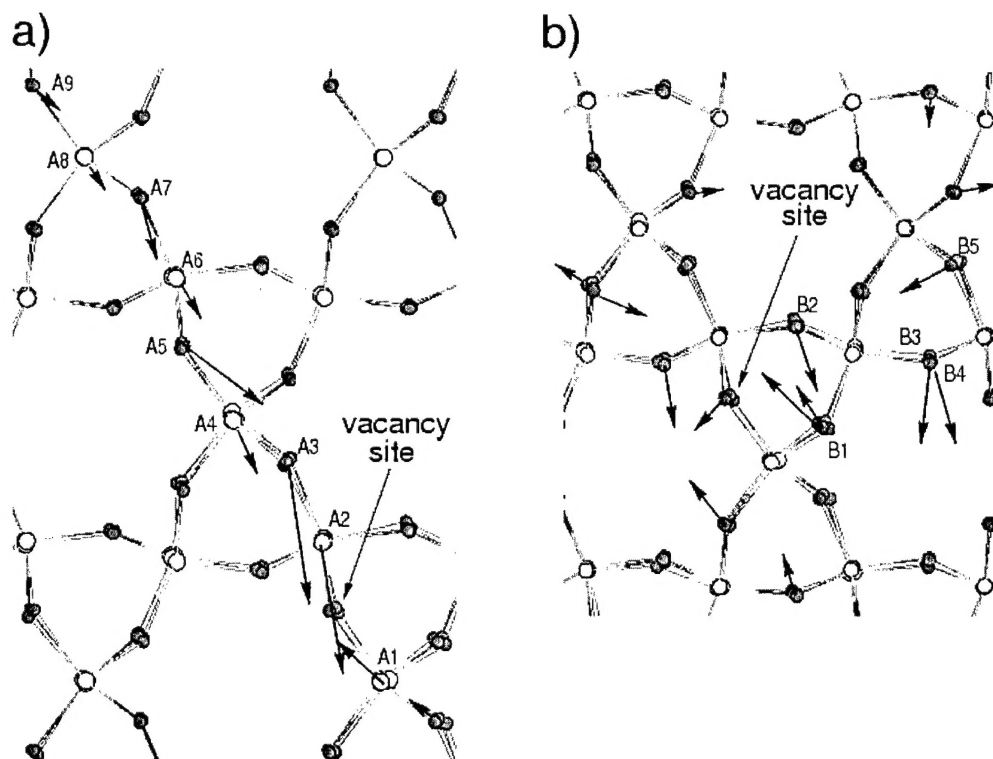


Figure 7. Projections of directions of atomic displacements near the vacancy (atoms are shown in their ideal lattice positions). The length of each arrow corresponds to the magnitude of the displacements scaled by four times for better visibility. Notations correspond to those in Figs. 6 and 3(b).

We calculated the optical excitation and luminescence energies of the neutral vacancy in the Franck-Condon approximation using several techniques. Calculations were performed for the defect geometries corresponding to the fully relaxed S_0 state ($S_0^* \rightarrow T_1$ in our Tables) and T_1 state ($T_1^* \rightarrow S_0$). In these notations (*) means a fully relaxed state. To calculate the excitation energies from the ground singlet state S_0 to the lowest triplet state T_1 and the luminescence energies from the relaxed triplet state we used a Δ SCF approach, i.e. taking the differences between the total energies of the system in the triplet and singlet states. To pinpoint excitations associated specifically with the bonding and anti-bonding orbitals of the vacancy site and estimate oscillator strength of dipole electronic transitions we used a configuration interaction technique which takes into account single-electron excitations (CIS)²⁵ as implemented in the Gaussian98 code²⁰. Finally, more accurate calculations for luminescence energies were carried out using a Coupled Cluster method with double excitations (CCSD)²⁶.

The optical transition energy of 7.6 eV calculated in the smallest cluster using CIS is in agreement with the observed strong absorption band at 7.6 eV attributed to the ODC(I) centre²⁷. However, we regard this agreement as fortuitous. As has been pointed out in ref.²⁸, neither the 6-31G basis set nor the CIS method is adequate for calculating optical properties of this defect due to importance of the electron correlation. In addition, we have shown that the results strongly depend on the cluster size and the extent of the lattice relaxation accounted for in calculations. Our results with extended basis sets nevertheless confirm that the optical absorption energy of the neutral vacancy in α -quartz should be larger than 5 eV. The small luminescence energy found in our calculations suggests that there is a high probability of a non-radiative $T_1^* \rightarrow S_0$ transition. Therefore we expect that the luminescence of this defect will be strongly suppressed.

4. Summary and conclusions

To summarise, we believe that the results of initial tests of the new method are very encouraging and demonstrate its ability to calculate the geometric and electronic properties of neutral and charged defects in silicon dioxide with good accuracy. This work presents the first comprehensive analysis of the full extent and character of the lattice relaxation around Oxygen vacancy in α -quartz, which was not possible to achieve using methods employed in previous studies. It has become possible because the embedded cluster method used here does not confine the defect-induced lattice relaxation to molecular cluster or periodic cell. We also predict the strong backward relaxation in the lowest triplet excited state of the vacancy and small (less than 1 eV) triplet luminescence energy of this defect.

Further work will focus on studies of other defect properties in quartz and on the development and application of the technique to defect studies in amorphous silica. We should note that the large radius of the lattice relaxation around the neutral vacancy in α -quartz found in this work should be characteristic to other defects, such as E' centres. The relaxation around these defects in amorphous silica is subject of our current investigations. The radius of relaxation is comparable or even larger than characteristic thickness of currently attainable oxide layers on silicon and dimensions of silica nano-crystals. This suggests that properties of these defects may strongly depend on their position with respect to surfaces of respective systems. The strong lattice deformation and the dipole moment of neutral vacancies should affect their interaction. Our results suggest that this interaction could be also affected by external electric field. Both effects could be relevant for performance of thin oxide films as gate dielectrics in microelectronic devices.

References

- ¹ M. Boero, A. Pasquarello, J. Sarntheim, and R. Car, Phys. Rev. Lett. **78**, 887 (1997).
- ² A. H. Edwards, Phys. Rev. B **36**, 9638 (1987).
- ³ M. Cook and C. T. White, Phys. Rev. B **38**, 9674 (1988).
- ⁴ A. Yokozawa and Y. Miyamoto, Appl. Phys. Lett. **73**, 1122 (1998).
- ⁵ J. K. Rudra and W. B. Fowler, Phys. Rev. B **35**, 8223 (1987).
- ⁶ A. L. Shluger and J. D. Gale, Phys. Rev. B **54**, 962 (1996).
- ⁷ A. L. Shluger, P. V. Sushko, and L. N. Kantorovich, Phys. Rev. B **59**, 2417 (1999).
- ⁸ P. V. Sushko, A. L. Shluger, and C. R. A. Catlow, Surface Sci. **450**, 153 (2000).
- ⁹ P. V. Sushko, A. L. Shluger, R. C. Baetzold, and C. R. A. Catlow, J. Phys.: Condens. Matter **12**, 8257 (2000).
- ¹⁰ B. G. Dick and A. W. Overhauser, Phys. Rev. **112**, 90 (1958).
- ¹¹ B. W. H. van Beest, G. J. Kramer, and R. A. V. Santen, Phys. Rev. Lett. **64**, 1955 (1991).
- ¹² These techniques have been reviewed in a special issue: C. R. A. Catlow and A. M. Stoneham (ed.) J. Chem. Soc. Faraday. Trans. II **85** (1989).
- ¹³ J. D. Gale, J. Chem. Soc. Faraday Trans. **93**, 69 (1997).
- ¹⁴ J. M. Vail, J. Phys. Chem. Solids **51**, 589 (1990).
- ¹⁵ A. L. Shluger, A. H. Harker, V. E. Puchin, N. Itoh, and C. R. A. Catlow, Modelling Simul. Mater. Sci. Eng. **1**, 673 (1993).
- ¹⁶ A. L. Shluger, A. I. Livshits, A. S. Foster, and C. R. A. Catlow, J. Phys. Condensed Matter **11**, R295 (1999).

- ¹⁷ J. Sauer, Chem. Rev. **89**, 199 (1989).
- ¹⁸ A. E. Reed, R. B. Weinstock, and F. Weinhold, J. Chem. Phys. **83**, 735 (1985).
- ¹⁹ B. Civalleri, C. M. Zicovich-Wilson, P. Ugliengo, V. R. Saunders, and R. Dovesi, Chem. Phys. Lett. **292**, 394 (1998).
- ²⁰ Gaussian98 (edition A7) M. J. Frisch, G. W. Trucks, H. B. Schlegel, G. E. Scuseria, M. A. Robb, J. R. Cheeseman, V. G. Zakrzewski, J. A. Montgomery, R. E. Stratmann, J. C. Burant, S. Dapprich, J. M. Millam, A. D. Daniels, K. N. Kudin, M. C. Strain, O. Farkas, J. Tomasi, V. Barone, M. Cossi, R. Cammi, B. Mennucci, C. Pomelli, C. Adamo, S. Clifford, J. Ochterski, G. A. Petersson, P. Y. Ayala, Q. Cui, K. Morokuma, D. K. Malick, A. D. Rabuck, K. Raghavachari, J. B. Foresman, J. Cioslowski, J. V. Ortiz, B. B. Stefanov, G. Lui, A. Liashenko, P. Piskorz, I. Komaromi, R. Gomperts, R. L. Martin, D. J. Fox, T. Keith, M. A. Al-Laham, C. Y. Peng, A. Nanayakkara, C. Gonzalez, M. Challacombe, P. M. W. Gill, B. G. Johnson, W. Chen, M. W. Wong, J. L. Andres, M. Head-Gordon, E. S. Replonge, and J. A. Pople, , Gaussian Inc. Pittsburgh PA, 1998).
- ²¹ P. E. Blöchl, Phys. Rev. B **62**, 6158 (2000).
- ²² V. B. Sulimov, P. V. Sushko, A. H. Edwards, A. L. Shluger, and A. M. Stoneham, Phys. Rev. B (submitted).
- ²³ H. B. Jansen and P. Ross, Chem. Phys. Lett. **3**, 140 (1969).
- ²⁴ A. Hamza, Á. Vibók, G. J. Halász, and I. Mayer, J. Molec. Struct. (Theochem) **501-502**, 427 (2000).
- ²⁵ J. B. Foresman, M. Head-Gordon, and J. A. Pople, J. Phys. Chem. **96**, 135 (1992).
- ²⁶ R. J. Rico and M. Head-Gordon, Chem. Phys. Lett. **213**, 224 (1993).
- ²⁷ L. Skuja, J. Non-Crystal. Solids **239**, 16 (1998).
- ²⁸ B. B. Stefanov and K. Raghavachari, Phys. Rev. B **56**, 5035 (1997).

Contract F61775-00-WE001**Title: First principle calculations of electrical levels for radiation induced defects in amorphous SiO₂**

This material is based upon work supported by the European Office of Aerospace Research and Development, Air Force Office of Scientific Research, Air Force Research Laboratory, under Contract No. F61775-00-WE001.

Any opinions, findings and conclusions or recommendations expressed in this material are those of the author(s) and do not necessarily reflect the views of the European Office of Aerospace Research and Development, Air Force Office of Scientific Research, Air Force Research Laboratory.

The Contractor, University College London, hereby declares that, to the best of its knowledge and belief, the technical data delivered herewith under Contract No. F61775-00-WE001 is complete, accurate, and complies with all requirements of the contract.

DATE: 21/08/2002**Name and Title of Authorized Official:**Dr. A. Shlyuger Ollie

I certify that there were no subject inventions to declare as defined in FAR 52.227-13, during the performance of this contract.

DATE: 21/08/2002**Name and Title of Authorized Official:**Dr. A. Shlyuger Ollie